



## Adaptive PID Control for 8/6 Switched Reluctance Motor Drive Based on BFO

Muhammed A. Ibrahim<sup>1,2\*</sup>, Ahmed Nasser B. Alsammak<sup>1</sup>

<sup>1</sup>Electrical Engineering Department, College of Engineering University of Mosul, Mosul 41001, Iraq

<sup>2</sup>System and Control Engineering Department, College of Electronics Engineering, Ninevah University, Mosul 41001, Iraq

Corresponding Author Email: [muhammed.ibrahim@uoninevah.edu.iq](mailto:muhammed.ibrahim@uoninevah.edu.iq)

<https://doi.org/10.18280/jesa.560403>

### ABSTRACT

**Received:** 20 March 2023

**Revised:** 20 August 2023

**Accepted:** 25 August 2023

**Available online:** 31 August 2023

#### Keywords:

*switched reluctance motor, PID controller, speed control, optimization*

The switched reluctance motor (SRM) has garnered considerable attention in both scholarly and industrial spheres due to its notable advantages such as the absence of rare earth materials and low manufacturing costs. However, the complexity of controlling SRMs, resulting from their nonlinear magnetization characteristics, remains a significant drawback. This paper presents a dual-pronged contribution. Firstly, it introduces a highly accurate and reliable model designed to evaluate the operational efficiency of a 4 kW 8/6 SRM. The magnetization characteristics have been optimized using the FEMM4.2 program in tandem with AutoCAD, which facilitates the selection of an optimal number of points for motor dimensions based on the finite element method. Secondly, the design of a proportional-integral-derivative (PID) controller for a nonlinear SRM is a complex task. Therefore, we have employed bacterial foraging optimization (BFO) to ascertain the optimal PID coefficients for controlling the speed of an SRM. Owing to its simplicity, ease of implementation, and high effectiveness, BFO is capable of delivering high-quality solutions, leading to a marked improvement in both transient and steady-state performances. The simulation results demonstrate that the control system approach utilizing PID-BFO exhibits the most desirable dynamic response characteristics.

## 1. INTRODUCTION

Increasing interest in the electrification of transportation results from the increased demand for clean and abundant energy sources. Due to the depletion of oil and the increase in its price, as well as the problem of air pollution caused by automobiles that rely on the internal combustion engine, there has been a recent surge in interest in electric vehicles (EVs) and their development (ICE). Therefore, the researchers are compelled to seek out new sources of energy for vehicle propulsion [1].

SRM drive system is a suggesting competitive in the application of variable speed drive because of its fault tolerance ability, simple construction and high efficiency. It is utilized in numerous engineering appliances, including wind generation systems, electric vehicle technology, etc. However, the complex nonlinearity of internal electromagnetic torque generated by the dual-salient in stator rotor poles and commutating an electric current in the stator supply side between phases affects the output speed response of the SRM complex to be controlled [2-4].

The schematic representation of the closed-loop speed control system for the SRM drive is shown in Figure 1. The controller is comprised of two loops. Speed controller in the outer loop. While a current controller is in the inner loop. The speed controller loop produces the commanded current ( $I_{ref}$ ) from the speed error. The commanded current ( $I_{ref}$ ) required is evaluated with the actual motor phase current ( $I_{ph}$ ) to evaluate the error signal of the current. This error signal is passed to a current controller to control the motor current and

follow its reference value by suitable gate signals to power converter circuit feeding the motor [5, 6].

Although there are numerous advantages associated with the SRM drive system, it is crucial to recognize the existence of several significant challenges that require investigation. The SRM drive system with nonlinearity is hard to achieve satisfying performances with conventional controllers as its parameters are nonadjustable. The torque quality and controller complexity issues are regarded as the most significant barrier to the widespread adoption of SRM for EV applications. However, these problems can be investigated and overcome. Therefore, several studies have been carried out over the past few years to attain critical performance characteristics of SRM drive utilization of different control methods.

To improve the performance of SRMs established on angle position controller, Chen et al. [7] implemented a fuzzy logic control (FLC) based on a mathematical model of the system for closed-loop rotor shaft speed regulation of the SRM drive. This is accomplished by adjusting the turn-on angle during the stator current commutation process. Rouhani et al. [8] compare two methods of controlling the SRM drive system. First, SRM drive control uses an adaptive neuro-fuzzy design. Afterwards, the methods for computing with neural networks are employed. The results show that the planned methods are appropriate for the intelligent control strategy of this barely nonlinear system behaviour. Using a radial basis function (RBF) neural network, Xia et al. [9] proposed an adaptive pulse width modulation (PWM) rotor speed regulator for SRM drive. This method uses the RBF neural network to build a rotor speed regulator with accurate estimating and quick

convergence. Elmas and Yigit [10] suggest a genetic algorithm-based proportional-integral (PI) rotor speed controller for the outer speed loop of the SRM drive. PC C++ software applied the genetic algorithm-based PI controller. TMS320F240 DSPs implement both SRM drive controllers. The genetic algorithm-based PI controller responds less to boundary changes and disruption. Using the fuzzy logic theory and the PI controller, Ongole [11] proposes a new method to achieve optimum control. In order to regulate the rotational speed of a machine, engineers use a fuzzy logic and proportional integral derivative (PID) system that automatically adjusts its parameters. To regulate and lessen the ripple of the stator current in the SRM drive, Li et al. [12] suggest a Fuzzy logic controller (FLC). The simulation results show that the planned method boosts the functioning of the SRM drive. It is achieved by compensating for the SRM current, which improves the performance of the SRM drive and the dynamic stability. Based on the fast terminal sliding mode control (FTSMC) method, Divandari et al. [13] suggest a novel speed controller structure for the (SRM) drive. Limited temporal convergence in the presence of external perturbation is guaranteed, which is a strength in addition to payload

disturbance and border reservations. The rotor speed response of the SRM is simulated and studied in MATLAB software. The genetic algorithm GA developed optimum H-Infinity regulator scheme is optimized by Meenakshi et al. [14]. The planned method's overall performance is more suited to improving the SRM drive's rotor speed control operation. To design the linear quadratic regulator with integral action (LQI), Souza et al. [15] investigate metaheuristic algorithms; a thorough comparison is made between the suggested algorithms and the PID controller; finally, the optimal method for controlling the Q and R coefficients in an SRM drive system is selected. The proposed control structures have been validated by simulation and experiment. Comparing the LQI + GA to the more common PID and LQI controllers reveals that the LQI + GA is more computationally efficient and has a faster response. The SRM model was built into the MATLAB software, and the PI regulator was introduced into the simulation environment. Multiple sets of simulation data demonstrate that the PI regulator can resolve the nonlinear difficulty of the SRM speed control system. It thereby reduces the oscillation frequency and overshoot of the control system, enhancing the drive system's stability and response [16].

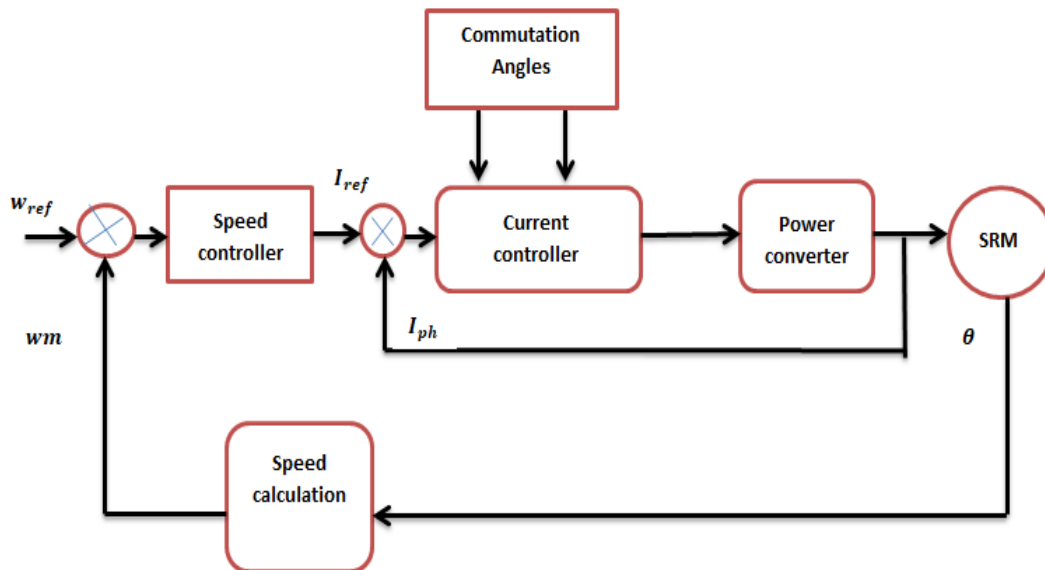


Figure 1. General feedback control system block diagram of the SRM

The previous literature review examines the variety of research conducted in the field of SRM drives. Despite the manifold benefits attributed to SRM, it is imperative to acknowledge the presence of several significant challenges that necessitate examination and investigation. The concise summary of contemporary advancements in SRM modelling, design, and control effectively highlights the significance of this motor in present-day technology. The motor under consideration exhibits highly non-linear magnetic characteristics. It poses significant challenges in developing an accurate SRM model and achieving superior dynamic performance especially concerning speed regulation systems.

Research scope in controller design is a challenging task for the SRM drive system. Hence, there exists a significant opportunity for research and development in the domain of controller design for the SRM drive system. Achieving high levels of reliability and accuracy across all operating points requires employing a motor representation model that closely approximates the actual system. This paper proposes a precise

speed controller based on an adaptive PID controller. BFO has tuned it for an 8/6, 4 kW four-phase SRM drive system. The BFO possesses notable attributes such as straightforwardness, simplicity in implementation, and a high level of effectiveness, enabling it to deliver excellent solutions. In the same manner, it assesses the dynamic performance of the intended controller. The inquiry is based on evaluating both steady-state and dynamic transient performance. The demonstration showcases the resilience of the designed controller.

## 2. MODELING AND MAGNETIC CHARACTERISTICS OF SRM

An accurate and appropriate model is crucial to any control system strategy. Various operational conditions characterize the process. Consequently, to accurately evaluate the performance of the SRM drive system and the effectiveness of

various control methods, it is imperative to have a reliable model of the SRM drive system.

A switching reluctance motor comprises a unipolar power converter and multi-phase salient poles in both the stator and the rotor of a variable reluctance machine. Figure 2 shows the machine structure of a four-phase 8/6 SRM. It has salient poles distributed as follows: six on the rotor and eight on the stator [17, 18].

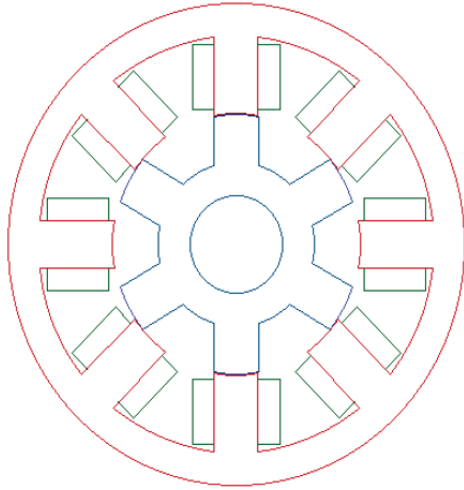


**Figure 2.** Four phases 8/6 switched reluctance motor structure

The machine is characterized by its inductance that varies in function of rotor position, as presented in Figure 3. The minimum inductance  $L_{min}$  corresponds to the unaligned position and maximum inductance  $L_{max}$  correspond to the alignment of the rotor and stator poles.

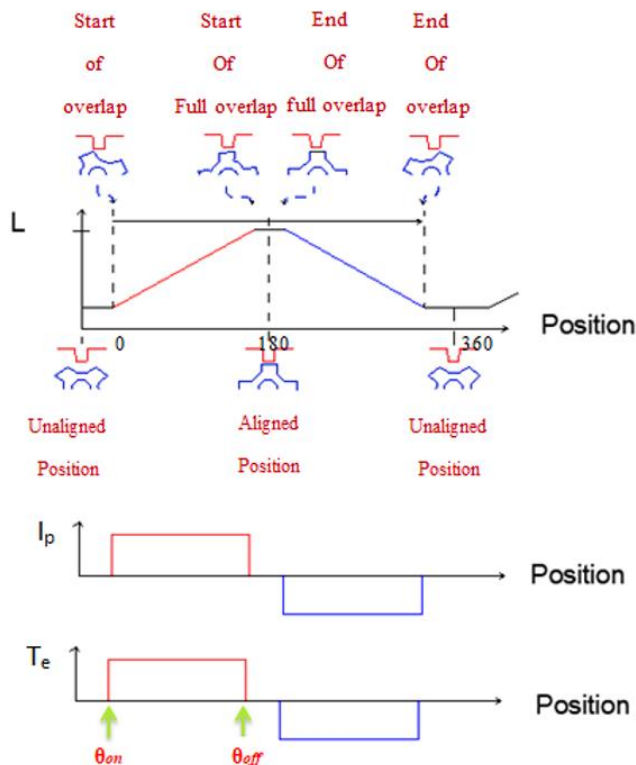


**Figure 3.** Variation of inductance and torque with rotor position

The excitation opening at an angle  $\theta_{on}$ , which is stated as the turn-on angle  $\theta_{on}$  and the angle when the demagnetization establishes is stated as the turn-off angle  $\theta_{off}$ . The stator winding is individually fed by a four-phase asymmetrical half-bridge converter as shown in Figure 4. The asymmetric bridge converter is the frequent and commonly utilized power converter for SRM drives due to offering good performance in quadrant operation.

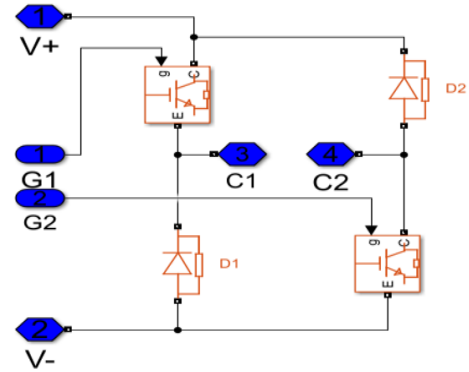


**Figure 4.** Per-phase asymmetric half bridge converter

In this work, an 8/6 SRM 4 kW is chosen. The details are examined and highlighted in studies [19, 20]. For the mechanical section of the 8/6 motor, the movement equation (Newton's law) and the voltage equations (Kirchhoff's law) are used as models. The voltage supplied by the power converter is applied to the eight phases of the six-by-six SRM. The flux linkage in each phase is determined by integrating the phase voltage minus the  $(R \times I)$  drop in the windings, as shown in [20]:

$$V = R_s i + \frac{d\lambda(\theta, i)}{dt} \quad (1)$$

The current lookup table can determine the resultant current for each phase. It takes the rotor position and the flux linkage as its inputs. By using the respective equations in conjunction with this resulting current and the rotor's actual position, one can determine the torque produced by each phase.

$$T_e(\theta, i) = \frac{\partial w(i, \theta)}{\partial \theta} \quad (2)$$

where,  $W$  magnetic co-energy is computed using the following equation:

$$W = \int \lambda(\theta, i) di \quad (3)$$

SRM's phase-decoupling allows static FEA simulations at different rotor positions with different phase current excitation to yield phase flux LUTs. Similarly, the generation of the torque LUT can also be achieved. The electromagnetic torque characteristic is pre-computed based on the FEMM4.2 software program and stored in a lookup table to expedite the simulation process. It takes place in the Simulink model. The values for the current and torque lookup tables are derived from the magnetization characteristic table. It can be found in Figure 5 of the 8/6 SRM model scheme in Simulink.

Figure 6 illustrates the current and torque lookup tables used in the 8/6 four phases SRM model.

The total electromagnetic torque generated on the motor's

rotor shaft is then determined by adding up the electromagnetic torques. It is produced by each of the four phases of the motor. The following movement equation governs both the mechanically dynamic component of the motor and the torque that is imparted to the load:

$$T_e = Bw + j \frac{dw}{dt} + T_L \quad (4)$$

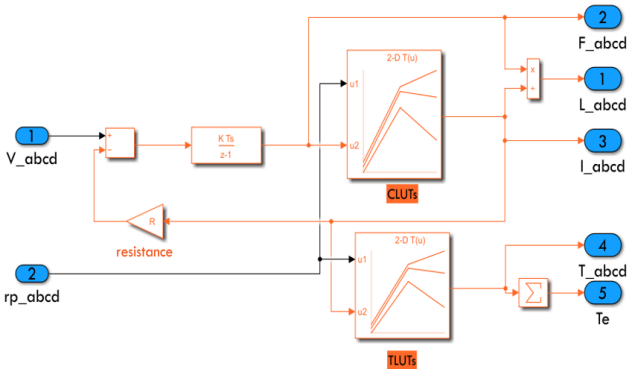
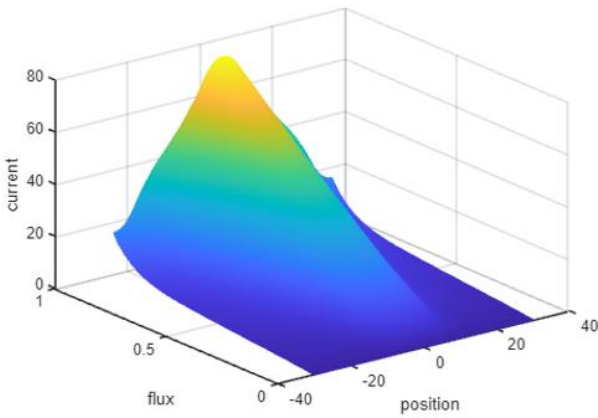
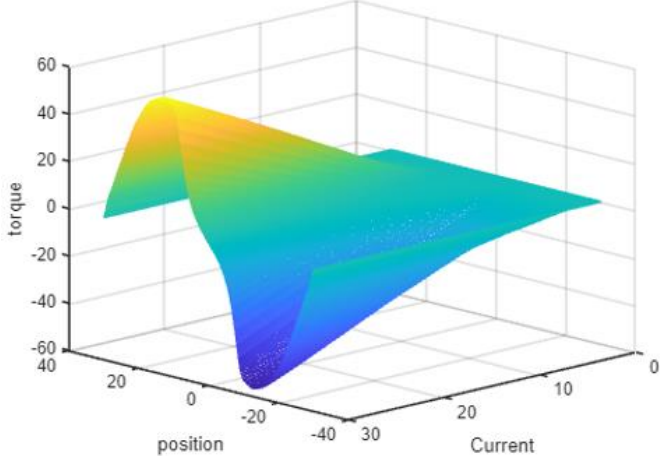


Figure 5. 8/6 SRM model scheme in Simulink



(a) Current(I), versus flux(λ), and rotor position(θ)



(b) Torque (Te), versus current(I), and rotor position(θ)

Figure 6. Magnetization lookup tables data in the SRM Simulink representation

### 3. CONTROL APPROACH

The employment of Proportional-Integral-Derivative (PID) control has gained significant traction in complex industrial settings where precise control of system dynamics is essential.

Proportional P, integral I and derivative D of the error indicator are united in a PID control. They provide specific enhancements for the full system dynamic response. The rotor speed controller intended for this paper is a PID controller. The deviation of the actual speed from the reference speed represents the speed error signal passed as input to the speed controller, and the output of the speed controller is the current command for the current controller. The differential equation regarding the PID controller dynamics can be stated as [21]:

$$C(t) = k_p + k_i \int e(t)dt + K_d \frac{d e(t)}{dt} \quad (5)$$

where,

- $e(t)$ : error signal
- $k_p$ : Proportional gain
- $k_i$ : Integral gain
- $k_d$ : Derivative gain

Determining the values of the  $(k_p, k_i, k_d)$  coefficients through analytical methods present challenges in achieving optimal control system operation with a given process. The utilization of manual methods may result in an excessive amount of time and potential harm when applied to actual hardware. For the above reasons, a programmable calculation mechanism is needed to reach the best solution with the simplest techniques. BFO will therefore be utilized for this purpose. BFO is a population-based optimization technique that is effective for global search methods [22].

In order to achieve simultaneous non-gradient optimization, the bacterial foraging optimization (BFO) method recreates the process by which bacteria hunt for nutrition in their surrounding environment. Kiven Passino points to the BFO in reference [23]. The significant concept of this algorithm is applying a group foraging strategy similar to that used by a swarm of E. coli bacteria in optimizing a multi-optimal function. Bacteria search for nutrients to maximise the energy they obtain in a given amount of time. Figure 7 depicts the configuration of the BFO modification PID controller factors [23].

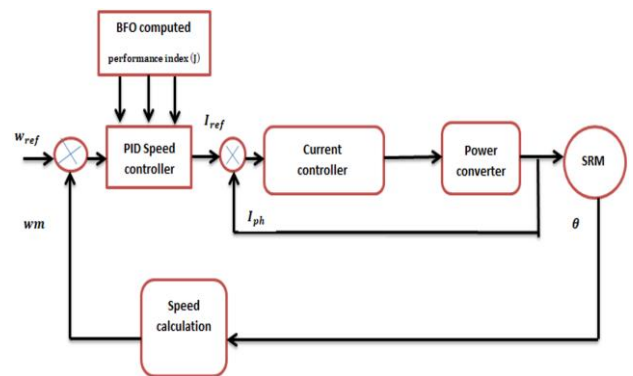


Figure 7. PID controller tuning configurations

To avoid the system production of the overshoot and fluctuation in dynamic response and generate the response to attain the reference signals required as soon as possible for reference tracking and external load disturbance rejection, the performance index is selected as below [24]:

$$\text{performance index (J)} = \int_0^t [\Delta\omega(t)]^2 dt \quad (6)$$

In each optimization process for PID controller design the performance index(J) is calculated by BFO using minimization target for all operating points in the SRM drive system. Figure 8 shows this proposed study's Pseudo code for BFO implementation [25].

```

Pseudo code for BFO
START
Initialize BFOA parameters
While (A termination situation has been satisfied)
  For loop (Elimination-dispersal (Ned))
    For loop (Reproduction (Nre))
      For loop (Chemotaxis (Nc))
        Run SRM drive system by Simulink call functions
        Compute fitness functions(performance index) P.

performance index (J) =  $\int_0^t [\Delta\omega(t)]^2 dt$ 
        Changes to the positions of control variables
      End loop (Chemotaxis)
      Calculate fitness values P
      based on fitness values, sort bacteria
      Copy the best solution (best bacteria position)
    End loop(Reproduction)
  Elimination and dispersal process with probability (Ped)
End loop (Elimination-dispersal)
End
  
```

Figure 8. Pseudo code for the proposed BFO implementation

#### 4. SIMULATION AND RESULT

This section provides an overview of the closed loop system with a proposed SRM drive controller utilizing the MATLAB/SIMULINK program. The system is examined in various operational contexts. The speed of the output rotor is detected and evaluated in relation to the desired set point speed. The error in the rotor speed signal is utilized as an input for the PID controller to generate a reference current that, when multiplied by the commutation angles, produces a gate drive signal suitable for the power converter.

For the various operating points in the SRM drive system, MATLAB/SIMULINK is used to examine the effectiveness of the intended methods. Reference tracking is vital in maintaining stability and accuracy in control systems. Continuously adjusting the system's quantity based on the difference between the reference signal and the actual output. One particular application where reference tracking is commonly utilized is in controlling motor speeds. When a square wave input is provided to a motor, tracking and matching its speed with this input waveform is essential. This ensures that the motor operates at the desired speed.

This section presents the typical motion profile with an acceleration, constant speed, and deceleration region to clarify the acceleration and deceleration torque. As opposed to load torque, acceleration torque is the necessary torque to accelerate an inertial load up to its reference speed or decelerate from a reference speed to a lower set. Figures 9, 10, and 11, respectively, show the effect of three different operating points on acceleration and deceleration error area when the SRM drive is under control based on an optimized PID controller.

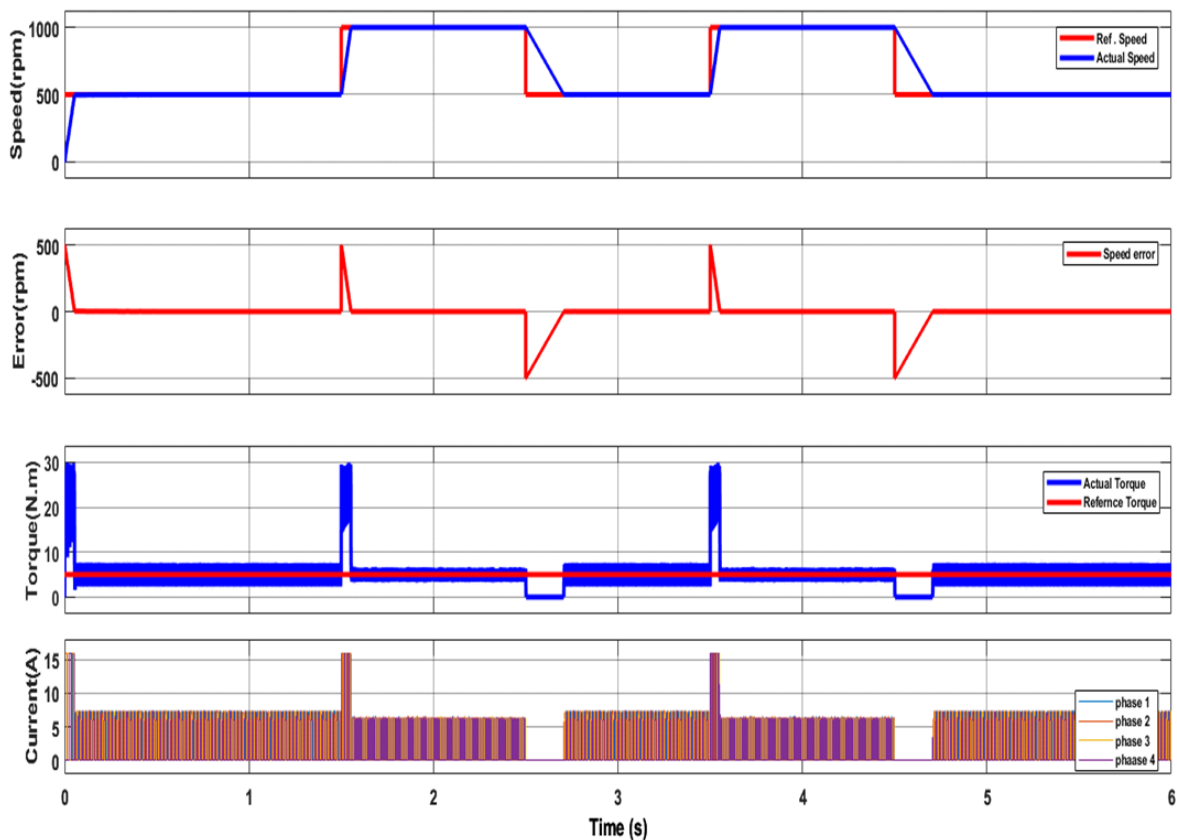


Figure 9. Speed response for square wave tracking 5 N.m load torque

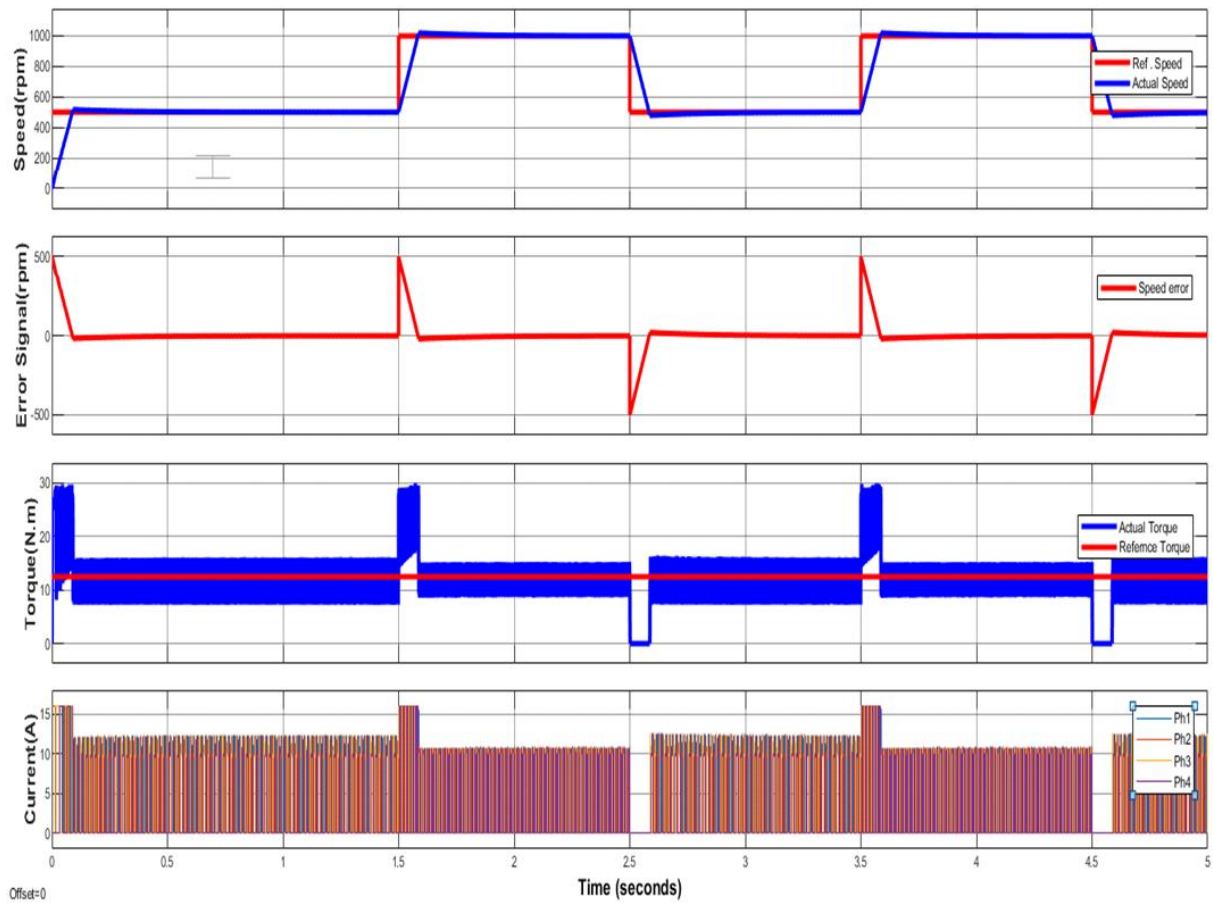


Figure 10. Speed response for square wave tracking 12.5 N.m load torque

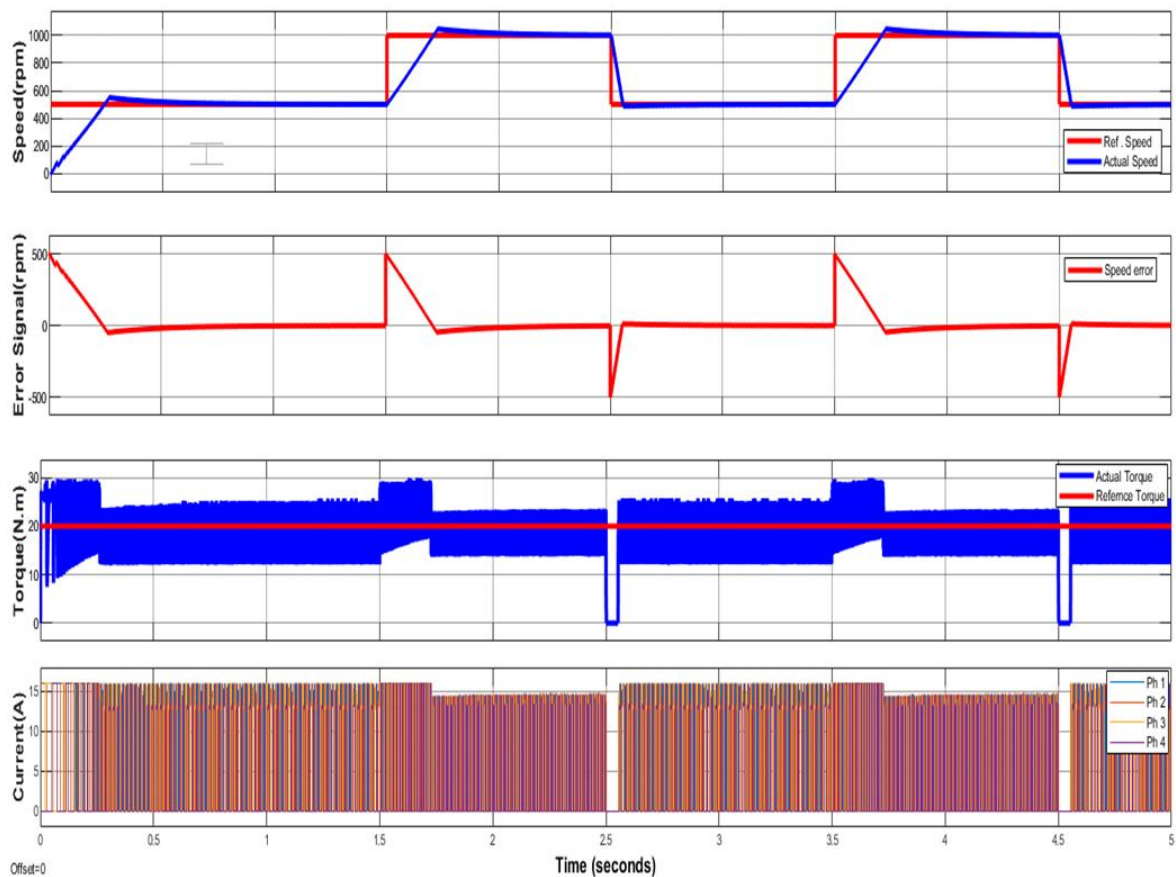
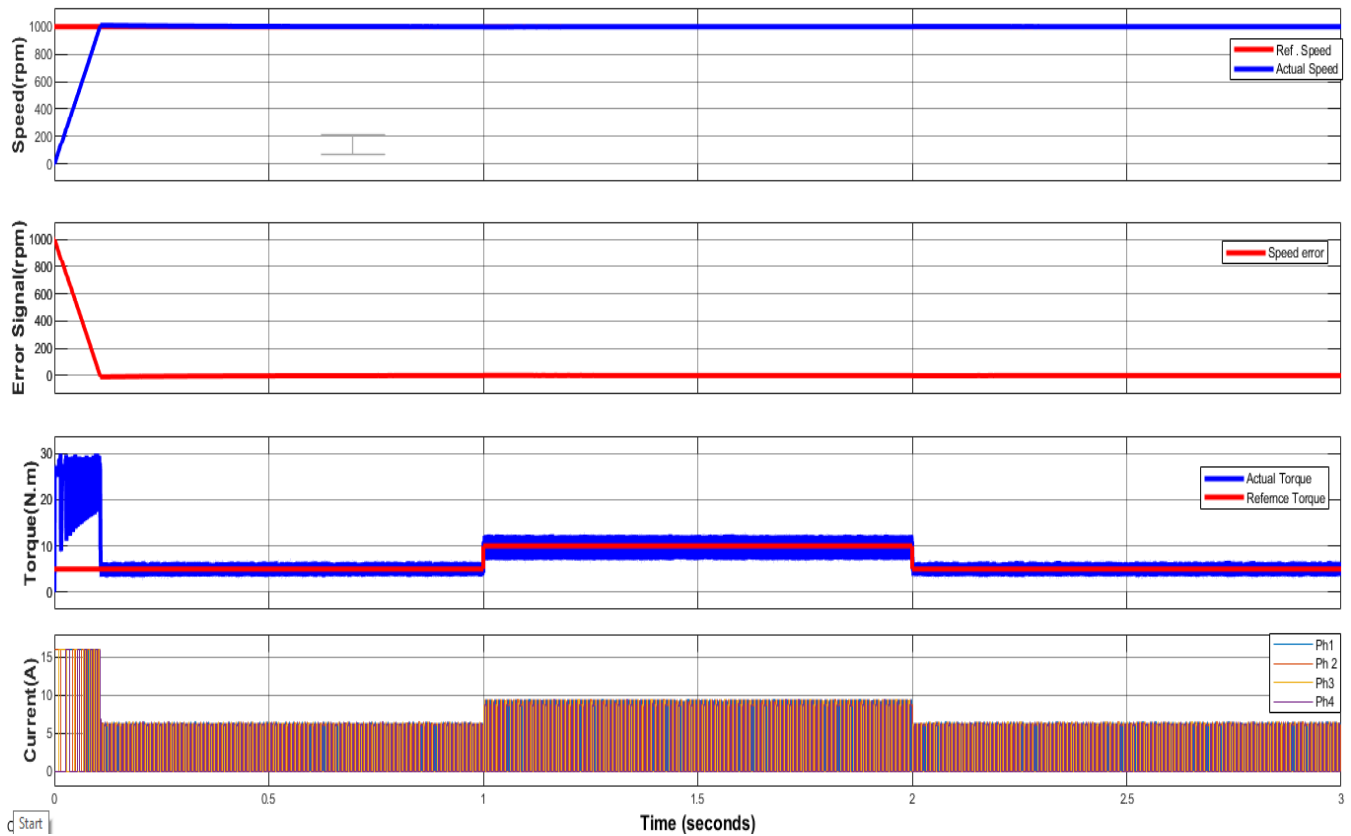


Figure 11. Speed response for square wave tracking 20 N.m load torque



**Figure 12.** The response of rotor speed with set point tracking (1000rpm) with load torque 10 N.m and 5 N.m

In order to test the antidisturbance ability of the adaptive PID controller based on BFO, the validation is carried out with a step change of external load torque during steady operation. The current, instantaneous torque, error signal, and rotor speed responses are shown in Figure 12. The load torque value is increased from 5 N.m to 10 N.m. The control system exhibits a notable level of dynamic performance. It can be observed that the control system can mitigate the effects of torque perturbation by making a minor adjustment to the current (and, consequently, the instantaneous torque). The rotational speed decreased to 1000 rpm, and within a time interval of 0.3 seconds, the system successfully restored the speed to its designated reference value.

## 5. CONCLUSIONS

For the 8/6 SRM drive system, the PID controller parameters are determined by adapting the objective function using the BFO algorithm. The controller is straightforward, simple, and easy to apply. Additionally, it is the cheapest price and the best speed response. The simulation results provide evidence to support the hypothesis that the planned PID controller will perform an adequate job of regulating the actual speed of the SRM drive. Because of the hard nonlinearity inherent in the SRM drive system, the BFO algorithm is used to determine the controller constants. The suggested controller offers accurate action for various square wave tracking and for rejecting various external load disturbances. Consequently, this intended controller is achievable for commercialized drive applications such as electric vehicles and aircraft. The controller has been designed with increased flexibility, with all stages of the control unit being programmed. In future,

learning-based approaches such as reinforcement learning can be implemented to control the SRM drive system dynamics.

## ACKNOWLEDGMENT

The authors are grateful to (Mosul University / College of Engineering) for their provided facilities that enhanced the quality of this work.

## REFERENCES

- [1] Boulanger, A.G., Chu, A.C., Maxx, S., Waltz, D.L. (2011). Vehicle electrification: Status and issues. *Proceedings of the IEEE*, 99(6): 1116-1138. <https://doi.org/10.1109/jproc.2011.2112750>
- [2] Li, C., Wang, G., Li, Y., Xu, A. (2018). Robust adaptive neural network control for switched reluctance motor drives. *Automatika*, 59(1): 24-34. <https://doi.org/10.1080/00051144.2018.1486797>
- [3] Vijayakumar, K., Karthikeyan, R., Paramasivam, S., Arumugam, R., Srinivas, K.N. (2008). Switched reluctance motor modeling, design, simulation, and analysis: A comprehensive review. *IEEE Transactions on Magnetics*, 44(12): 4605-4617. <https://doi.org/10.1109/tmag.2008.2003334>
- [4] Bilgin, B., Jiang, J.W., Emadi, A. (2019). Switched reluctance motor drives: Fundamentals to applications. CRC Press. <https://doi.org/10.1201/9780203729991>
- [5] Krishnan, R. (2017). Switched reluctance motor drives: Modeling, simulation, analysis, design, and applications. CRC Press. <https://doi.org/10.1201/9781420041644>

- [6] Hamouda, M., Számel, L. (2018). Reduced torque ripple based on a simplified structure average torque control of switched reluctance motor for electric vehicles. In 2018 International IEEE Conference and Workshop in Obuda on Electrical and Power Engineering (CANDO-EPE), Budapest, Hungary, pp. 000109-000114. <https://doi.org/10.1109/CANDO-EPE.2018.8601133>
- [7] Chen, H., Shao, Z., Zhu, Y. (2004). Rotor speed testing and closed-loop control for switched reluctance motor drive based on fuzzy logic. In Fifth World Congress on Intelligent Control and Automation (IEEE Cat. No. 04EX788), 5: 4458-4462. <https://doi.org/10.1109/wcica.2004.1342358>
- [8] Rouhani, H., Milasi, R.M., Lucas, C. (2005). Speed control of switched reluctance motor (SRM) using emotional learning based adaptive controller. In 2005 International Conference on Control and Automation, Budapest, Hungary, pp. 330-334. <https://doi.org/10.1109/ICCA.2005.1528140>
- [9] Xia, C., Chen, Z., Xue, M. (2006). Adaptive PWM speed control for switched reluctance motors based on RBF neural network. In 2006 6th World Congress on Intelligent Control and Automation, 2: 8103-8107. <https://doi.org/10.1109/WCICA.2006.1713552>
- [10] Elmas, C., Yigit, T. (2007). Genetic algorithm based on-line tuning of a PI controller for a switched reluctance motor drive. *Electric Power Components and Systems*, 35(6): 675-691. <https://doi.org/10.1080/15325000601139674>
- [11] Ongole, A.P. (2015). Implementation of intelligent controller based current control strategy for SRM drive. *International Journal of Hybrid Information Technology*, 8(12): 349-354. <https://doi.org/10.1080/15325000601139674>
- [12] Li, C., Wang, G., Fan, Y., Bai, Y. (2016). A self-tuning fuzzy PID speed control strategy for switched reluctance motor. In 2016 Chinese Control and Decision Conference (CCDC), Yinchuan, China, pp. 3084-3089. <https://doi.org/10.1109/ccdc.2016.7531512>
- [13] Divandari, M., Rezaie, B., Ranjbar Noei, A. (2019). Speed control of switched reluctance motor via fuzzy fast terminal sliding-mode control. *Computers and Electrical Engineering*, 80: 106472. <https://doi.org/10.1016/j.compeleceng.2019.106472>
- [14] Meenakshi, S., Suresh Kumar, P., Ramsanjay, S. (2020). Soft computing techniques based digital adoptive controllers with intelligent system for switched reluctance motor. *International Journal of Advanced Science and Engineering*, 7(1): 1614-1624. <https://doi.org/10.29294/ijase.7.1.2020.1614-1624>
- [15] Souza, D.A., de Mesquita, V.A., Reis, L.L.N., Silva, W.A., Batista, J.G. (2020). Optimal LQI and PID synthesis for speed control of switched reluctance motor using metaheuristic techniques. *International Journal of Control, Automation and Systems*, 19(1): 221-229. <https://doi.org/10.1007/s12555-019-0911-x>
- [16] Zhang, C., Chen, K., Yu, J., Zhang, Q., Huo, C. (2022). Simulation analysis of SR motor speed regulation system based on PI control. *Journal of Physics: Conference Series*, 2268(1): 012009. <https://doi.org/10.1088/1742-6596/2268/1/012009>
- [17] Cajander, D., Le-Huy, H. (2006). Design and optimization of a torque controller for a switched reluctance motor drive for electric vehicles by simulation. *Mathematics and Computers in Simulation*, 71(4-6): 333-344. <https://doi.org/10.1016/j.matcom.2006.02.025>
- [18] Al Quraan, L., Szamel, L., Hamouda, M. (2021). Optimum switching angles control of SRM for electric vehicle applications. *Periodica Polytechnica Electrical Engineering and Computer Science*, 65(4): 394-403. <https://doi.org/10.3311/ppce.17640>
- [19] Hamouda, M., Számel, L. (2019). Accurate magnetic characterization based model development for switched reluctance machine. *Periodica Polytechnica Electrical Engineering and Computer Science*, 63(3): 202-212. <https://doi.org/10.3311/ppce.14012>
- [20] Parsapour, A., Dehkordi, B.M., Moallem, M. (2015). Predicting core losses and efficiency of SRM in continuous current mode of operation using improved analytical technique. *Journal of Magnetism and Magnetic Materials*, 378: 118-127. <https://doi.org/10.1016/j.jmmm.2014.10.148>
- [21] Ibrahim, M.A., Alsammak, A.N.B. (2022). Switched reluctance motor drives speed control using optimized PID controller. *Przeglad Elektrotechniczny*, 98(11): 48-52. <https://doi.org/10.15199/48.2022.11.07>
- [22] Zhang, G.Y., Wu, Y.G., Tan, Y.X. (2013). Bacterial foraging optimization algorithm with quantum behavior. *Journal of Electronics and Information Technology*, 35(3): 614-621. <https://doi.org/10.3724/sp.j.1146.2012.00892>
- [23] Das, S., Biswas, A., Dasgupta, S., Abraham, A. (2009). Bacterial foraging optimization algorithm: Theoretical foundations, analysis, and applications. *Studies in Computational Intelligence*, 23-55. [https://doi.org/10.1007/978-3-642-01085-9\\_2](https://doi.org/10.1007/978-3-642-01085-9_2)
- [24] Ibrahim, M., Khather, S. (2020). Optimized PID controller for a self-lift positive output Luo-converter. *Proceedings of the Proceedings of the 1st International Multi-Disciplinary Conference Theme: Sustainable Development and Smart Planning, IMDC-SDSP 2020, Cyperspace*, 28-30 June 2020. <https://doi.org/10.4108/eai.28-6-2020.2298084>
- [25] Passino, K.M. (2005). *Biomimicry for optimization, control, and automation*. Springer Science & Business Media. <https://doi.org/10.1007/b138169>